Astronomical and Astrophysical Transactions (*AApTr*), 2026, Vol. 36, Issue 1, pp. 19–30,
ISSN 1055-6796, Photocopying permitted by license only, ©Cambridge Scientific Publishers

Coupled variations of polar motion and the geomagnetic field over the past century

A.E. Volvach*, G.S. Kurbasova, L.N. Volvach

Department of Radio Astronomy and Geodynamics, Crimean Astrophysical Observatory, Katsively, RT-22 Crimea

Received 30 September, 2025; accepted 30 September, 2025

This study investigates coherent relationships between the Earth's polar motion and variations in the geomagnetic field over the past century. Using two-channel autoregressive analysis at reference coordinates (90°N, 0°W), statistically significant correlations are identified between annual changes in the Earth's mean pole (IERS) and the geomagnetic field intensity vector (IGRF-14). A quasi-periodic signal with a period of approximately 25 years is detected, with geomagnetic variations leading changes in the mean pole by about 2.5 years. In addition, a 3.3-year periodicity is simultaneously observed in year-to-year variations of the geomagnetic dipole moment and polar motion parameters. The analysis also reveals coherent epochs characterized by extreme events, including jumps and turning points, occurring in both systems. These empirical results support the possibility of a dynamic coupling between Earth's rotation and the evolution of its geomagnetic field.

Keywords: Mean pole, Earth, secular variations, IGRF calculator

1 Introduction

By the end of the last century, the movement of the Earth's poles had finally been established. The shift of the poles changes the geographical coordinates of places on the Earth's surface, affects the determination of time and affects a number of astronomical, geodesical, geophysical and climatological tasks (Dickey et al. 2011, Hide and Dickey 1991). For the collection and prompt analysis of data on the Earth's North Pole motion in 1899, the International Latitude Service was created, renamed in 1961 as the International Polar Motion Service (IPMS). Currently, any problems of pole movement are the responsibility of the International Earth Rotation and Reference Systems Service, IERS.

The rotation of the Earth and the movement of its poles is characterized by a complex process of orientation changes. The excitation of these changes and their geophysical consequences in various fields have not been fully studied and are currently

*Email: a.volvach@gmail.com

the subject of research (Hide and Dickey 1991, Vondrak and Ron 2014, Vondrak and Ron 2015).

One of these unexplored problems is a change in the orientation of the motion in the Northern mean pole over the surface of the Earth, shown by the turning points on the graphs of the polhodes (the plane with the axis of the pole x_p, y_p).

In the process of studying the causes of changes in orientation in the Earth's North Pole movement, it becomes necessary to match these changes with various geophysical processes, in particular, with changes in the positions of geomagnetic poles, since it is believed that a geomagnetic field is generated inside the Earth (Braginsky 1984, Reshetnyak 2013, Fournier et al. 2015, Roberts 2007). This suggests that the same global processes that affect the Earth's rotation, also affect the geomagnetic field.

Recently published papers (Vondrak and Ron, 2014, 2015) showed that the appearance of jumps in magnetic field data correlates with changes in the Earth's rotation parameters. These results confirm the fact of unity within the Earth processes generating a geomagnetic field, and a change in the Earth's rotation parameters. The establishment of coherent variations in this case contributes to the creation of reliable physical models of cause–effect relationships.

2 A source of data on the movement of the Northern mean pole of the Earth

For analysis, we used data on the movement of the Northern mean pole in the IERS definitions from 1900 to 2016 (http://hpiers.obspm.fr/eoppc/eop/eopc01/mean-pole.tab). In the IERS definition, gravitational field models include the tesseral harmonics coefficients C21 and S21. These parameters describe the position of the axis of the figure of the Earth relative to the ground coordinate system. In this case, the axis should coincide with the observed position of the pole of rotation averaged over the same period of time. The ground coordinates of the mean axis of rotation in the IERS model can be considered as a long-term trend obtained after filtering Chandler's fluctuations and seasonal components for the period from 1900 to 2016.

The coordinates of the mean pole are annually updated and published in the annual reports of the IERS service (IERS Annual Report 2011, 2012, 2013: http://www.iers.org). One of the latest plots of the long-term trend of the Earth's North Pole of the Earth IERS is shown in Figure 1. The graph shows a non-linear trend that shows the return points and their location in time.

3 A source of data on the Earth's geomagnetic North pole motion

In contrast to Earth's two geographic poles, usually considered four poles characterizing the Earth's magnetic field: 2 geomagnetic and 2 magnetic. At present, the southern magnetic pole is in the Earth's Northern Hemisphere, and the northern magnetic pole is in its Southern Hemisphere. However, the poles are generally called in accordance with the hemisphere in which each of them is located.

Changes in the main geomagnetic field don't occur quickly but they are able to be modeled mathematically, for example in the International Geomagnetic Reference

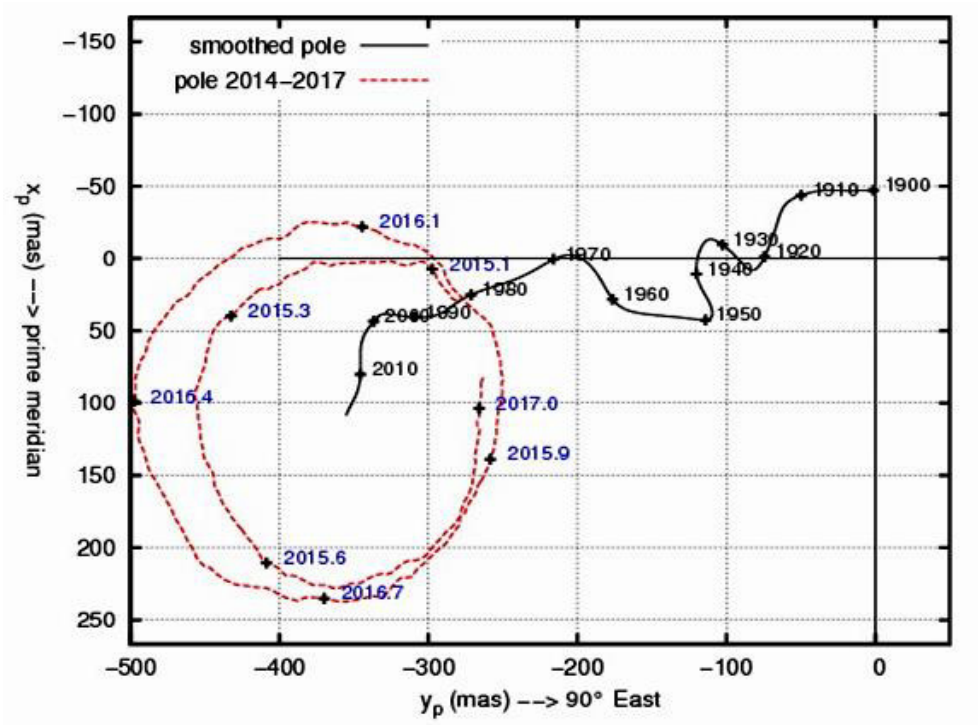


Figure 1 IERS definition of the movement of the Northern mean pole from 1900 to 2014 and the polhode of IERS. The period of measurements is from 2014 to 2017 and coordinates are shown in arc seconds (mas). Image source: http://hpiers.obspm.fr/eoppc/eop/eopc01/mean-pole.jpg.

Field (IGRF) and the WMM main field models (Thébault et al. 2015). The International Geomagnetic Field (IGRF) is a mathematically modeled and still ongoing sequential dataset starting from 1900 that describes the large-scale interior of our planet's magnetic field.

Based on the coefficients of the WMM2015v2 model for 2019.0, the geomagnetic North Pole is located at 72.69° West and 80.61° North, while the South Geomagnetic Pole is at 107.31° East and 80.61° South. At present the dipole's axis is tilted 9.45° to the axis of the Earth's spin. This dipole can be used as a simplified geomagnetic coordinate system (Thébault et al. 2015). Based on the IGRF-12 model, the positions of the geomagnetic and magnetic poles are updated. Figure 2 shows graphs of the movement of geomagnetic and magnetic poles over the last century.

Since the geomagnetic field is a vector one, minimally three components are needed to describe it. Components characterizing the field's direction: declination D, slope I. Values D and I are measured in units of angular degrees. D – the angle between the horizontal component and the direction to the geographic North Pole, I – the angle between the horizontal plane and the intensity vector of the general field. The elements characterizing the field strength: vertical component Z total intensity F, horizontal component H, as well as horizontal intensity components aimed to the

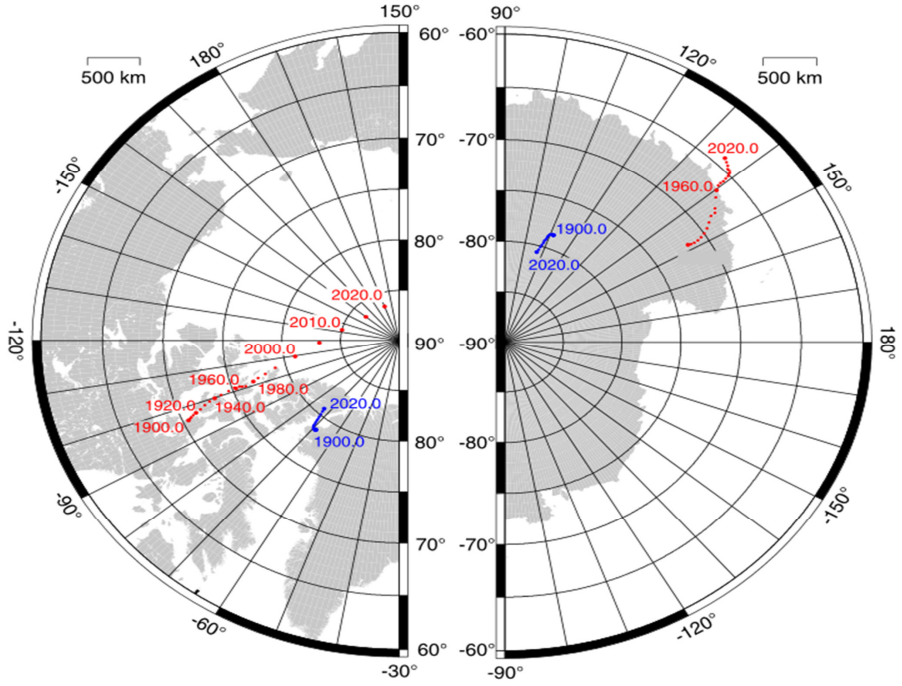


Figure 2 The movement of the magnetic pole (red) and the geomagnetic pole (blue) since 1900 according to IGRF-12 in the Northern Hemisphere (left) and the Southern Hemisphere (right). Stereographic projection is used. The scale shows the distance on the ellipsoid WGS84, that is true along the lines of constant longitude, as well as along the lines of mid-latitudes. The source of the figure (Thébault et al. 2015, p.16).

North X and East Y, are connected by the following basic equations (Thébault et al., 2015):

$$F = \sqrt{X^2 + Y^2 + Z^2} = \sqrt{H^2 + Z^2}, \tag{1}$$

$$H = F \cdot \cos(I), \quad Z = F \cdot \sin(I), \quad X = H \cdot \cos(D), \quad Y = H \cdot \sin(D). \tag{2}$$

For analysis, we used data on the parameters of the North geomagnetic pole calculated with the IGRF14 calculator (NGDC Geomagnetic Calculators).

4 Discussion

4.1 Features on the graphs of data on motion parameter variations of the mean pole of the Earth

In further analysis, by features we mean short-term variations in the sign of the first derivative and its return to the previous level of values, or a short-term transition to

another level (Arnold, 1992, p. 2). On the graph of multi-year displacement of the mean pole (see Fig. 1), the direction of the pole displacement locally changes at the return points. In this case, a full return to the previous level does not occur. We calculate the trends in the change in the distance of the mean North Pole from the conditional beginning according to IERS data (graph in Fig. 3a).

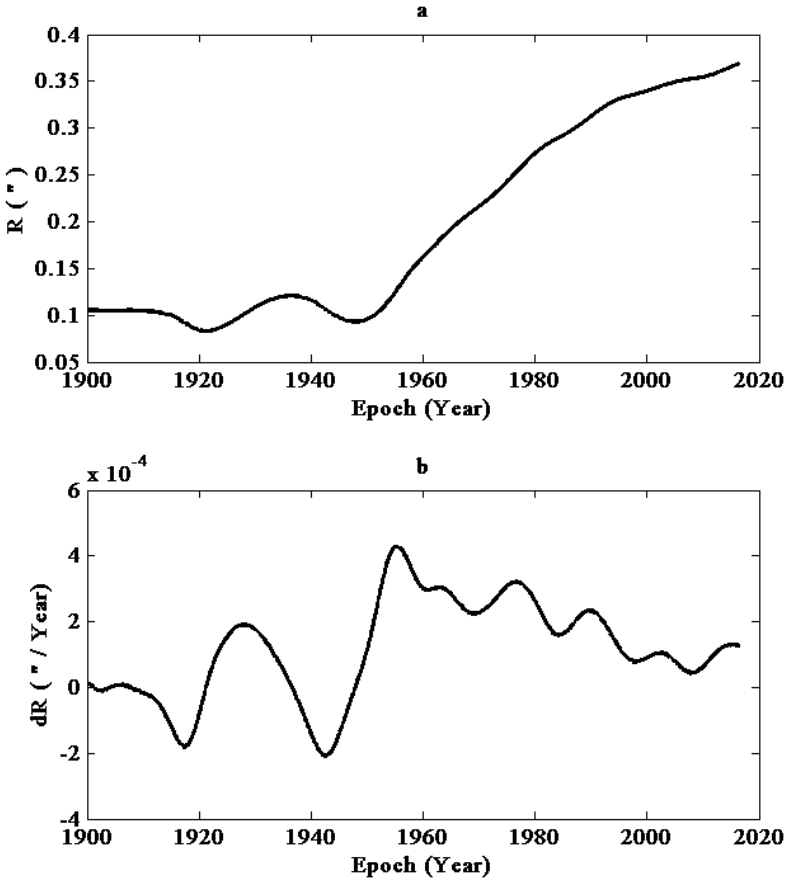


Figure 3 Distances from the conditional beginning $R = \sqrt{x_p^2 + y_p^2}$ (a) and changes in dR from year to year (b) for the period 1900–2016.

Figure 3a shows an increase in distance R after 1948, while changes in this distance from year to year dR – decrease (Fig. 3b). Let us compare the trends in the change in the position of the Earth's mean pole with secular variations of the geomagnetic field.

4.2 Secular variations of the geomagnetic field

The Earth's magnetic field changes gradually over a period lasting several to thousands of years (Yang et al. 2000). Such changes are called secular variations of the

geomagnetic field (Latyshev et al. 2017, Fournier et al. 2015). Secular variations except slowly changing also prone to short-term spikes (Arnold et al. 2012, p. 11). Relatively sharp change of secular variations speed of Earth's geomagnetic field parameters (one or more) called geomagnetic jump (see Fig. 4).

The French scientists (Courtillot and Le Mouël 1984, Courtillot et al. 1978) initially noticed this phenomenon. At numerous stations where magnetic readings are taken they realized that the trend in secular changes before 1969 is decidedly different from those afterwards. This tendency, that is more visible in the eastern part of the magnetic field at stations in Europe, was witnessed at many stations situated on different continents as well. Geophysicists associate the acceleration of the North geomagnetic pole with the geomagnetic jump that occurred in 1969-1970 (Thébault et al. 2015).

Until about 1971, the North Geomagnetic Pole shifted uniformly at a speed of about 9 km/year, then suddenly began to accelerate (see Fig. 5).

Secular changes of the geomagnetic declination at a location with geodetic coordinates of 90° latitude north, 0° longitude west for the period from 1900 to 2019 were calculated using the declination calculator (NGDC Geomagnetic Calculators, https://www.ngdc.noaa.gov/geomag/calculators/magcalc.shtml?model=igrf). A smooth model and a graph of secular variations in geomagnetic declination was constructed based on the results of these calculations. When choosing the type of model corresponding to the most accurate statistical criteria for approximation, the approximation model of the Fourier series in trigonometric form turned out to be the most suitable. To select

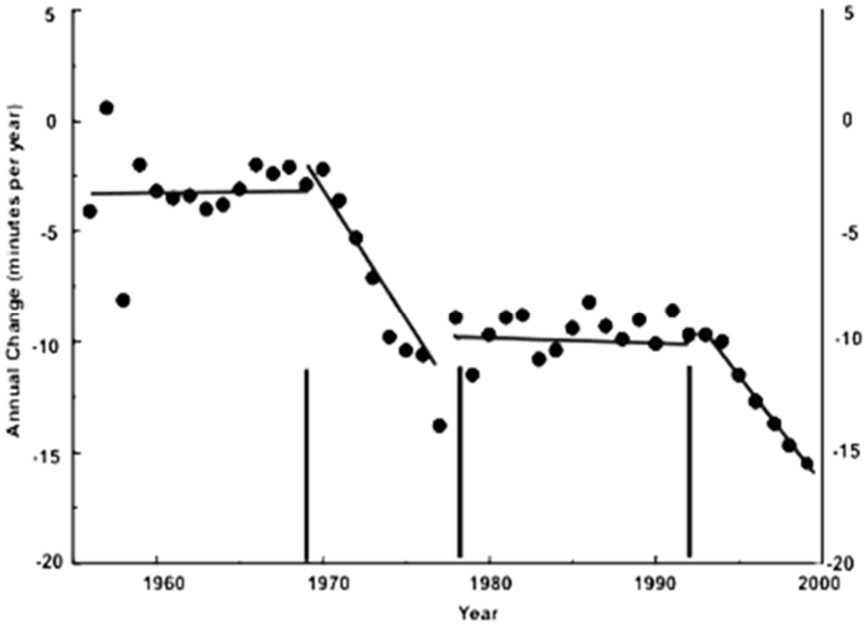


Figure 4 Annual changes in geomagnetic declination at the Midpole Magnetic Observatory, north of Edmonton (http://geomag.nrcan.gc.ca/magfld/sec-en.php).

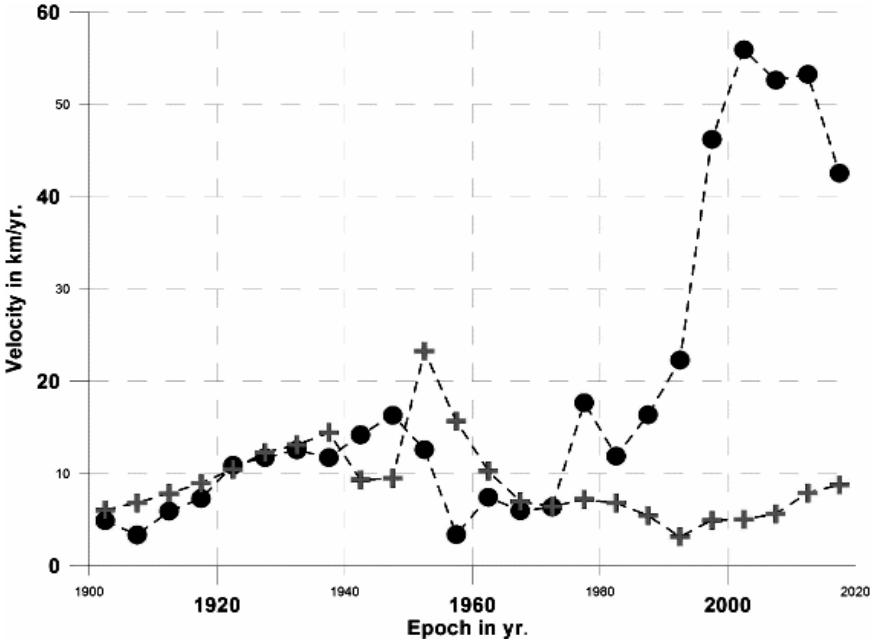


Figure 5 Northern element of the geomagnetic pole speed in the southern hemisphere (crosses) and northern hemisphere (balls) evaluated on a spheroid WGS84 (Thébault et al. 2015, p. 17.

the optimal type of model and method for optimizing the approximation process, we used the resources presented in the field of mathematical and software MATLAB-11 (https://www.mathworks.com/). As a result, the model is selected:

$$f(x) = a_0 + a_1 \cdot \cos(xw) + b_1 \cdot \sin(xw) + a_2 \cdot \cos(2xw) + b_2 \cdot \sin(2xw), \qquad (3)$$

where the coefficients (with a 95% confidence interval – a range of values within which the coefficient value is a 95% probability) are:

$a_0 = 0.5637$ (0.5017, 0.6256);
$a_1 = 0.11$ (–0.0159, 0.2369);
$b_1 = -0.6221$ (–0.7245, –0.5197);
$a_2 = -0.4334$ (–0.4859, 0.3808);
$b_2 = -0.08039$ (–0.2427, –0.08188);
$w = 0.03993$ (0.03722, 0.04264).

Coefficient a_0 models a constant term in the data, units of measurement for the coefficients (°/year), w corresponds to the signal's main frequency, $n = 2$ corresponds to the amount of terms (harmonics) in the approximated data.

In this model, the argument x is counted in units (year) relative to the beginning of the approximate time series of data. Frequency $w = 2\pi/P$, where $P = 157.4$ years. In assessing the accuracy indicators for approximating the data of curve (3),

the two most important are the following values: RMSE = 0.1698 – standard error or standard error of approximation; $R^2 = 0.8944$ is the square of the correlation between the initial and predicted values (a value close to 1 indicates that the model factors in a large proportion of the difference). Figure 6 show that long-term trend changes secular variation of the geomagnetic field declination increases since 1970 and has an irregular tendency. The return points correspond to the maximum and minimum values of function (Eq. 3) in 1912, 1942, 1973, 2018 (Volvach et al. 2022).

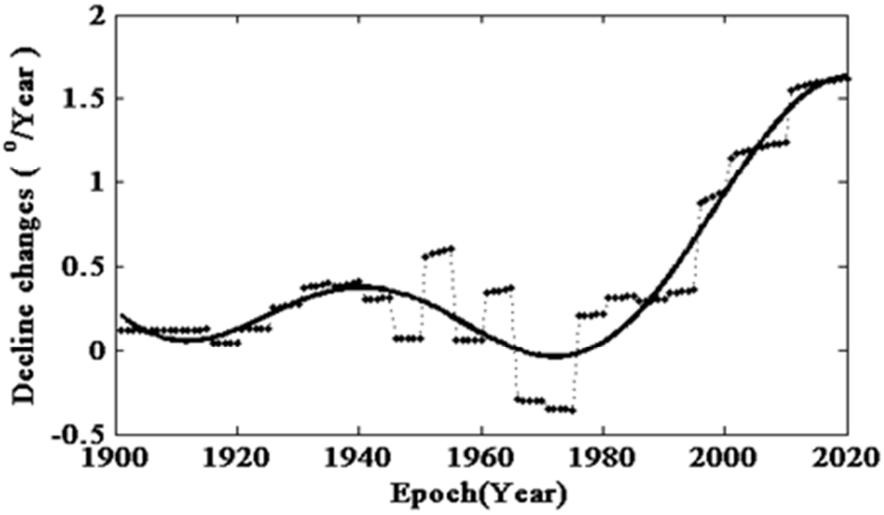


Figure 6 A graph of data on the yearly change of geomagnetic declination at a geodetic coordinates of 90° latitude north, 0° longitude west from 1900 to 2019 (marked with asterisks) and the approximation curve of these data using the model (continuous line).

A more accurate space-time arrangement of the jumps in the data dD will be obtained using the wavelet transform. For the wavelet approximation, Haar wavelets recommended in the case of a step signal were used (https://www.mathworks.com/). Figure 7 shows the spatio-temporal localization of the most significant jumps in magnitude in 1965, 1975, 1996.

Comparing the graphs of the tendencies of the displacement of the Earth's mean pole (Fig. 3a), changes in secular differences in geomagnetic declination dD (Fig. 6) as well as the increase in the speed of the geomagnetic pole's Northern element in the Northern Hemisphere (Fig. 5), we find their coincidence in sign (positive). After comparing trends in changes in secular differences in geomagnetic declination dD (Fig. 6) along with the speed of the Northern element of the North Geomagnetic Pole (Fig. 5), a concurrent accelerated growth was observed after 1970, while accelerated distance growth is observed after 1948. We use the method of two-channel autoregression analysis to assess the coherent relationship between the individual variations in the data dR and in the data on changes in the geomagnetic field characteristics at geodesic coordinates of 90° latitude north, 0° longitude west.

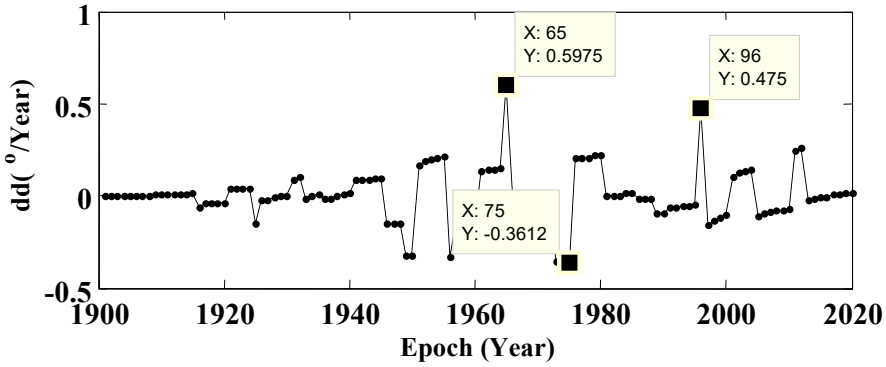


Figure 7 Graph of differences *dd* between the initial data and the wavelet approximation.

4.3 Establishment of coherent relationships

The spectral estimation method is a method of approximating data by one or more accepted statistical models. In cases where the amount of data is large enough, classical spectral estimates will be the most structurally stable spectral estimates. Moreover, the only assumption that is required for them is that the analyzed data should be stationary in the broad sense. The hundred year interval we use to analyze time series is a limited part of the complete time sequence of data. This led to the need to use alternative methods and models under the assumption that short data segments, obtained in practice from a longer data record, can be considered locally stationary. Attempts to reduce this problem to an easier and practically solvable one led to the use of various models of spectral power density (SPD), the algorithms and programs of which are given in a modern textbook (Marple 1987). The class of time series models that give rational SPD functions (AR – autoregression, ME – moving average and ARME – modeling sinusoids in white noise) is typical. These models are determined by some finite small set of coefficients. The result is less biased spectral estimates with higher resolution.

The class of the AR model used by us was established during the machine implementation of various models of spectral estimation of natural time events (sequence of sunspots, deviations of the day length from standard, changes in solar and climatic parameters, etc.). The advantages of this model include the fact that autoregressive spectra have sharp peaks, which is usually associated with high resolution. In addition, estimates of the AR parameters can be obtained by solving linear equations. Main characteristics of the selected model: class of ratings – parametric; model name – autoregressive (AR); methods – Yula-Walker and Berg (optional); quadratic form of the spectrum (definitions of the vector and matrix are given in (Marple 1987); the order of the AR model is used to control the relationship between resolution and dispersion.

According to this method, the establishment of a mutual correlation between two (single-channel) processes consists in obtaining the function of the mutual (two-channel) power spectral density, i.e. mutual correlation function of discrete-time Fourier transform (Marple 1987):

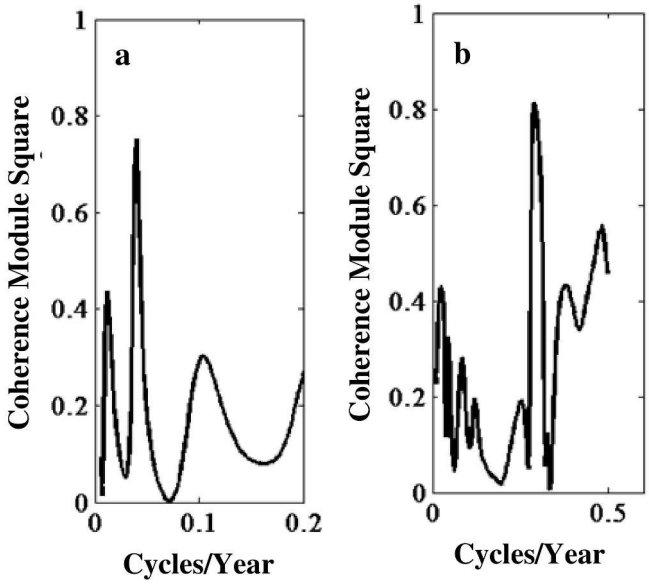


Figure 8 Coherence between annual changes in the mean pole vector (dR) and annual changes: a) vector of total intensity (dF) at the geodetic coordinates of 90° north latitude, 0° west longitude; b) vector of geomagnetic dipole moment ($dDIP$).

$$P_{xy} = T \cdot \sum_{k=-\infty}^{k=+\infty} r_{xy}[k] e^{-j2\pi f k T}, F_{xy} = \frac{P_{xy}(f)}{\sqrt{P_{xx}(f)}\sqrt{P_{yy}(f)}}, \tag{4}$$

where x, y are single-channel processes; f, frequency; T, time interval.

In (Eq. 4) to measure the similarity (as a function of frequency) of two signals, we calculate the square of the coherence module (SCM) (Marple 1987):

$$SCM(f) = |F_{xy}|^2, \tag{5}$$

and phase coherence spectrum

$$\theta(f) = \arctan\left[\frac{Im\{F_{xy}(f)\}}{Re\{F_{xy}(f)\}}\right]. \tag{6}$$

The size of the SCM (Eq. 5) is between 0 (for frequencies at which there is no consistency between the channels) and 1 (for frequencies at which the channels are completely coherent). The coherence phase (Eq. 6) characterizes the lag or phase advance of an event in channel x with respect to an event in channel y.

Let us analyze the results of applying this method of spectral estimates to identify coherent variations: between annual changes in the vector of the mean pole dR and annual changes: a) a vector of general intensity dF at geodetic coordinates of 90° latitude north, 0° longitude west (NGDC Geomagnetic Calculators https://www.ngdc.noaa.gov/geomag/calculators/magcalc.shtml?model=igrf); b) the vector of the geomagnetic dipole moment $dDIP$ (Magnetic North, Geomagnetic and Magnetic Poles. http://wdc.kugi.kyoto-u.ac.jp/poles/figs/pole-ns.tab).

The SCM graph in Fig. 8a shows a high coherence (SCM = 0.75) between differences over a 25 year timescale in the data dR and dF. In this case, the coherence phase is 2.5 years: a variation with a period of 25 years in the data dR is ahead of a similar variation in the data dF.

In the data dR and $dDIP$ with high reliability (SCM = 0.79) a coherence was established (Fig. 8b) between variations with a period of 3.3 years in data dR and $dDIP$. Moreover, variation with a period in the $dDIP$ data is ahead of a similar variation in the dR data.

5 Conclusions

Based on high-precision observations of the motion of the Earth's pole, the effects of the relationship of changes in the Earth's rotation parameters in era of magnetic jumps were discovered. Correlation processes in Earth's different spheres allows the synchronization of external and internal mechanically moving and reproducible events. The comparability of the time intervals of the appearance of jumps in the data on geomagnetic declination and turning points on the graph of the mean pole of the Earth allows these events to be correlated.

Using a two-channel autoregression analysis, a correlation was found between the annual changes in the Earth's mean pole vector (IERS) and the annual changes in the general intensity vector (IGRF-14) at a location with geodetic coordinates of 90° latitude north, 0° longitude west. Moreover, coherent variation with a period of 25 years in the data is ahead of a similar variation in the data by 2.5 years. In addition, as a result of the AR analysis, there is a correlation between the variations with a period of 3.3 years in the year to year changes of the data on the values of the geomagnetic dipole moment and in the data on the change in the position of the mean pole.

The establishment of coherent relationships and a comparison of the epochs of the appearance of extreme events (jumps and turning points) in the parameters of the geomagnetic field and the Earth's mean pole is based on empirical data. Nevertheless, the obtained results allow the possibility of a coordinated movement of two poles (the Northern mean pole of the Earth and the geomagnetic one), which is possible if there is a real connection between Earth's rotation and changes in Earth's geomagnetic field.

References

Arnold V.I. (1992) Catastrophe Theory, p. 129, Springer-Verlag Berlin Heidelberg.

Arnold V.I., Gusein-Zade S.M., Varchenko A.N. (2012) Singularities of Differentiable Maps, Volume 1 Classification of Critical Points, Caustics and Wave Fronts, p. 282, Springer.

Braginsky S.I. (1984) Geophysical & Astrophysical Fluid Dynamics, 30, 1, 1-78.

Courtillot V., Ducruix J., Le Mouël J.-L. (1978) C.R. Acad. Sci. Paris, D287, pp. 1095-1098.

Courtillot V., Le Mouël J.-L. (1984) Nature, 311, 709-716.

Dickey J.O., Steven L.M., Olivier de Viron (2011) Journal of Climate, 24, 569—574.
Dickman S.R. (2000) ASP Conference series, 208, 411-435.
Fournier A., Aubert J., Thébault E. (2015) Earth Planets and Space, 67, 81, 1-17.
Hide R., Dickey J.O. (1991) Science, 253, 629-637.
Latyshev A.V., Kushlevich D.O., Ponomareva V.V., Pevzner M.M., Fedyukin I.V. (2017) Izv., Phys. Solid Earth, 53, 750-759.
Marple S.L. (1987) Digital spectral analysis with applications, pp. 512, Englewood Cliffs, NJ, Prentice-Hall, Inc.
Reshetnyak M.Y. (2013) Three-dimensional domino model in geodynamo, Izv., Phys. Solid Earth, 49, 464-473.
Roberts P.H. (2007) Theory of the Geodynamo, Treatise of Geophysics, 2nd edn, Vol. 8, pp. 67–105, ed. Schubert, G., Elsevier.
Thébault E., Finlay C.C., Beggan C.D., et al. (2015) International Geomagnetic Reference Field: the 12th generation, Earth Planet Sp., 67, 79, 1-19.
Vondrak J., Ron C. (2014) Acta Geodyn. Geomater., 11, 3 (175), 1-8.
Vondrak J., Ron C. (2015) Earth orientation and its excitations by atmosphere, oceans, and geomagnetic jerks, Serbian Astronomical Journal, 191, 59-66.
Volvach A., Kurbasova G., Volvach L. (2022) Advances in Space Research, 69, 12, 4228-4239.
Yang S., Odah H., Shaw J. (2000) Variations in the geomagnetic dipole moment over the last 12000 years, Geophys. J. Int., 140, 158-162.